Hearing Research 345 (2017) 30–42

Contents lists available at ScienceDirect

Hearing Research

journal homepage: www.elsevier.com/locate/heares

Research Paper

Simultaneously-evoked auditory potentials (SEAP): A new method for concurrent measurement of cortical and subcortical auditory-evoked activity

Christopher Slugocki [a], Daniel Bosnyak [a], Laurel J. Trainor [a, b, *]

[a] Department of Psychology, Neuroscience & Behaviour, McMaster University, Hamilton, Ontario, Canada
[b] Rotman Research Institute, Baycrest Hospital, Toronto, Ontario, Canada

ARTICLE INFO

Article history:
Received 8 August 2016
Received in revised form
7 December 2016
Accepted 16 December 2016
Available online 31 December 2016

Keywords:
Auditory-evoked potentials (AEP)
Corticofugal
Auditory state-state response (ASSR)
Frequency-following response (FFR)
Brainstem
Cortex

ABSTRACT

Recent electrophysiological work has evinced a capacity for plasticity in subcortical auditory nuclei in human listeners. Similar plastic effects have been measured in cortically-generated auditory potentials but it is unclear how the two interact. Here we present Simultaneously-Evoked Auditory Potentials (SEAP), a method designed to concurrently elicit electrophysiological brain potentials from inferior colliculus, thalamus, and primary and secondary auditory cortices. Twenty-six normal-hearing adult subjects (mean 19.26 years, 9 male) were exposed to 2400 monaural (right-ear) presentations of a specially-designed stimulus which consisted of a pure-tone carrier (500 or 600 Hz) that had been amplitude-modulated at the sum of 37 and 81 Hz (depth 100%). Presentation followed an oddball paradigm wherein the pure-tone carrier was set to 500 Hz for 85% of presentations and pseudo-randomly changed to 600 Hz for the remaining 15% of presentations. Single-channel electroencephalographic data were recorded from each subject using a vertical montage referenced to the right earlobe. We show that SEAP elicits a 500 Hz frequency-following response (FFR; generated in inferior colliculus), 80 (subcortical) and 40 (primary auditory cortex) Hz auditory steady-state responses (ASSRs), mismatch negativity (MMN) and P3a (when there is an occasional change in carrier frequency; secondary auditory cortex) in addition to the obligatory N1-P2 complex (secondary auditory cortex). Analyses showed that subcortical and cortical processes are linked as (i) the latency of the FFR predicts the phase delay of the 40 Hz steady-state response, (ii) the phase delays of the 40 and 80 Hz steady-state responses are correlated, and (iii) the fidelity of the FFR predicts the latency of the N1 component. The SEAP method offers a new approach for measuring the dynamic encoding of acoustic features at multiple levels of the auditory pathway. As such, SEAP is a promising tool with which to study how relationships between subcortical and cortical processes change through early development and auditory learning as well as by hearing loss and aging.

1. Introduction

Auditory-evoked potentials (AEPs) are often used to non-invasively examine auditory processing dynamics in human listeners (Chandrasekaran et al., 2014). Acoustic transduction via the inner ear initiates volleys of synchronous neural depolarization along the auditory pathway. Under certain conditions, the post-synaptic potentials generated by populations of depolarizing neurons will summate and create propagating fluctuations in voltage that can be measured at the listener's scalp using electroencephalographic (EEG) electrodes. Averaging the EEG signal evoked over multiple stimulus presentations effectively attenuates spontaneous neural activity and increases the signal-to-noise ratio for those EEG potentials specifically evoked by the acoustic stimulus: the AEPs. A number of so-called “components,” can be identified in the human AEP, the exact combination of which depends largely on the properties of the acoustic stimulus, presentation parameters, and task of the listener (Luck, 2005).

Of relevance to the current study, different components have been attributed to functionally discrete stages of auditory processing and, most notably, localized to different subcortical and

* Corresponding author. Department of Psychology, Neuroscience & Behaviour, McMaster University, 1280 Main Street West, Hamilton, Ontario, L8S4L8, Canada.
E-mail address: LJT@mcmaster.ca (L.J. Trainor).

http://dx.doi.org/10.1016/j.heares.2016.12.014
0378-5955/

Abbreviations

AC	Auditory Cortex
AEP	Auditory-evoked Potential
ANF	Auditory Nerve Fiber
ASSR	Auditory Steady-state Response
CN	Cochlear Nucleus
DFT	Discrete Fourier Transform
DRC	Digital Room Correction
EEG	Electroencephalogram
FFR	Frequency-following Response
IC	Inferior Colliculus
IIR	Infinite Impulse Response
MMN	Mismatch Negativity
SEAP	Simultaneously-evoked Auditory Potentials
SLM	Sound Level Meter
TDT	Tucker-Davis Technologies
TTL	Transistor-transistor Logic

cortical generator sites along the auditory pathway (Eggermont, 2007). There is thus potential for AEP methods to measure how sound information is represented and transformed as it ascends the auditory neuraxis. However, to date, relatively few studies have examined subcortical and cortical AEP components from the same listeners and only some have made efforts to limit between-subject and/or between-session variability by recording subcortical and cortical components simultaneously in individuals (Bidelman, 2015b; Bidelman et al., 2014a, 2014b, 2013; Bidelman and Alain, 2015; Krishnan et al., 2012; Musacchia et al., 2008; Shiga et al., 2015; Sohmer and Feinmesser, 1970; Tietze, 1979; Woods et al., 1993). Therefore, the relationship between cortical and brainstem components remains unclear.

Developing methods for concurrent brainstem-cortical AEP measurement would be particularly useful experimentally for elucidating the neural dynamics involved in auditory learning as well as clinically for lesion detection and differential diagnosis of hearing loss. For example, recent research suggests that auditory learning results in changes to the way sound is encoded at subcortical nuclei below the level of auditory cortex (AC). In humans, much of this research is focused on the frequency-following response (FFR) owing to its potential as an index of acoustic feature representation in human subcortex (Skoe and Kraus, 2010a). The FFR is thought to reflect population-level synaptic activity from nuclei primarily within the rostral brainstem, namely the inferior colliculus (IC), which phase-locks to the periodicity of the evoking acoustic stimulus (Chandrasekaran and Kraus, 2010; Smith et al., 1975, 1978; Sohmer et al., 1977; Worden and Marsh, 1968), though it may also contain significant activity from auditory nerve (Bidelman, 2015a) and, at least for FFRs below 100 Hz, activity from cortical generators (Coffey et al., 2016). As a convergence hub, IC is the target of many ascending and descending projections within the auditory system (Winer, 2005). A wide variety of neural cell types with unique discharge patterns populate the IC and, together, are capable of representing complex auditory signals with high temporal precision (Peruzzi et al., 2000). This precision is partly reflected in the fidelity of the FFR signal, which can represent periodicity in the evoking stimulus up to at least 1000 Hz (Chandrasekaran et al., 2014; Kraus and Nicol, 2005). Crucially, human FFR data reveal patterns of morphological change which correlate with acoustic experience, such as with music or language (Bidelman et al., 2011; Krishnan et al., 2005, 2008, 2009, 2010a, 2010b; Krizman et al., 2012; Skoe and Kraus, 2013; Wong et al., 2007) as well as with short-term acoustic training (Anderson et al., 2013; Carcagno and Plack, 2011; Russo et al., 2005; Song et al., 2008) and real-time statistical learning (Skoe et al., 2013; Skoe and Kraus, 2010b). Insofar as the FFR primarily reflects the activity of subcortical nuclei, these experience-dependent effects complement a considerable body of research showing similar individual- and group-level effects in the morphology and topography of both transient and sustained components attributed to cortical generators. For example, the obligatory N1 and P2 transients—often localized to generators in secondary AC (Engelien et al., 2000; Godey et al., 2001; Picton et al., 1999)—stay neuroplastic into adulthood and can be enhanced following auditory training (Shahin et al., 2003; Tremblay et al., 2001; Tremblay and Kraus, 2002) as well as passive exposure to acoustic stimuli (Ross and Tremblay, 2009). Additional transient components generated outside of primary AC, such as the mismatch negativity (MMN) and P3a, also exhibit sensitivity to passive exposure, short-term training, and long-term acoustic experience such as with music and language (Atienza et al., 2004; Näätänen, 2008; Nikjeh et al., 2009; Uther et al., 2006). These so-called novelty-detection potentials are typically associated with the auditory-oddball paradigm wherein an infrequent sound or sequence of sounds is presented pseudo-randomly in an otherwise repetitive sound stream. The MMN is thought to reflect automatic auditory deviance-detection processes localized to secondary AC (Näätänen et al., 2007; Picton et al., 2000), whereas the P3a appears to reflect alerting processes in frontal lobe triggered when novel auditory features cause an involuntary reorienting of attention (for a review see: Polich, 2007; Yamaguchi and Knight, 1991). Responses from primary AC are also affected by experience. Cortical auditory steady-state responses (ASSRs), elicited by amplitude modulating a carrier signal at or around 40 Hz (Galambos et al., 1981; Ross et al., 2000), exhibit phase advancement in adult listeners following both auditory training and passive exposure (Bosnyak et al., 2004, 2007; Gander et al., 2010). The 40 Hz ASSR predominantly reflects activity in primary AC, with additional contributions from thalamus, thalamocortical circuits, and brainstem (Herdman et al., 2002).

One possibility is that corticofugal projections allow AC to modulate activity and/or plastic processes at subcortical nuclei to enhance biologically-relevant spectro-temporal features of the impinging sound (Suga et al., 2000, 2002; Suga, 2008; Suga and Ma, 2003; Wu and Yan, 2007; Zhou and Jen, 2007). An emerging literature questions whether such a feedback network can be measured in human listeners, but current evidence from concurrent recording of subcortical and cortical AEPs, though promising, remains inconclusive. For example, Musacchia et al. (2008) found that experience (i.e. musicianship) not only affected the morphology of components from both levels of the auditory hierarchy, but also modulated how strongly subcortical (FFR) and cortical (P1-N1) components were related. Similarly, Krishnan et al. (2012) found that a measure of pitch saliency in the subcortical FFR correlated with the magnitude of a late cortical potential elicited by stimuli containing cues to pitch. Further both subcortical and cortical representations of pitch processing predicted behavioral pitch discrimination limens better than either component alone. Bidelman et al. (2014b) failed to find a correlation between the morphology of early cortical components (i.e. P1-N1) and the subcortical FFR, but did find that the amplitude of the later cortical P2 component was significantly correlated with FFR encoding of the evoking speech signal's first formant frequency. The correlation between brainstem FFR and P2 was also stronger in young adult musicians compared to age-matched non-musicians. However, a subsequent study in older adult musicians found that the combined morphology of early cortical components (N1-P2 peak-to-peak

amplitude) together with the strength of the subcortical FFR predicted performance on a categorical speech task better than the morphology of either level alone (Bidelman and Alain, 2015).

Some ambiguity in the aforementioned studies may be attributable to differences in recording methodology. Concurrent measurement of AEPs from multiple levels of the auditory pathway involves finding a compromise between the optimal parameters for eliciting cortical and those for eliciting subcortical components. Cortical AEPs require slow presentation rates due to stark refractory effects (Davis et al., 1966; Picton et al., 1977). For example, N1 amplitude increases dramatically—by 5.6 μV—for every tenfold increase in inter-stimulus interval (ISI) from 0.5 to 3 s (Nelson and Lassman, 1968). Conversely, brainstem generators are relatively unaffected by reductions in ISI down to about 10 msec (Ballachanda et al., 1992), though an ISI of 50 msec is considered ideal for recording subcortical FFR (Bidelman, 2015b). Brainstem AEP components also need to propagate through more tissue relative to cortical AEPs before reaching the scalp. Hence, the subcortical components are smaller in amplitude than cortical components and require averaging over a higher number (~2000) of trials to achieve an acceptable signal-to-noise ratio (SNR). Accurate recording of the FFR signal up to 1500 Hz further requires an EEG amplifier capable of sampling scalp voltage at a much higher rate than required to faithfully capture cortical AEPs whose response morphology can be represented using sampling rates as low as 100 Hz (Burkard et al., 2007). This raises concerns about computer processing power and data storage when stimulus duration and ISI are extended for optimal recording of cortical components.

Some studies (Krishnan et al., 2012; Musacchia et al., 2008) have used a relatively short ISI (~500 msec) to find a balance between the optimal ISI for recording cortical responses and the time required to simultaneously collect a sufficient number of trials to visualize subcortical components. This approach cuts down on overall recording time, but attenuates early cortical components such as P1, N1, and P2 relative to recordings using longer ISIs. Others (e.g. Bidelman et al., 2014a, 2014b; Bidelman and Alain, 2015) have used a blocked design wherein cortical responses are collected in a block where stimuli are presented with a long ISI and subcortical responses are collected in a separate block where stimulus presentation is rapid. Clustered presentation further refines the blocked design by presenting stimulus clusters, where each stimulus is separated by a short ISI, at longer intervals in order to measure a robust cortical response to the first stimulus in each cluster (Bidelman, 2015b). Though blocked and clustered designs allow for optimal recording of subcortical and cortical components within a single experimental session, neither approach results in true simultaneous measurement.

In the present study, we propose a new method termed Simultaneously-evoked Auditory Potentials (SEAP) as a tool with which to examine the relationship between concurrently-elicited subcortical and cortical AEP components. Central to the SEAP method is a stimulus consisting of a pure-tone carrier frequency (500 Hz) that is amplitude-modulated at the sum of 37 and 81 Hz. The stimulus is 512 msec in duration with a 500 msec ISI and presented to participants monaurally through a calibrated acoustic transmission line over 2400 trials at a fixed polarity. At random, for 15% of trials, the carrier frequency is changed from 500 to 600 Hz. The SEAP method should be able to evoke all AEP components reviewed above. First, presentation of a fixed polarity stimulus with a 500 Hz carrier frequency over 2070 trials should suffice to elicit a detectable FFR at 500 Hz in the averaged AEP (Krishnan, 2007; Thornton, 2007). Further, because the acoustic transmission line increases the separation of the transducer from the recording electrodes, the FFR trace should offer an artifact-free index of spectro-temporal feature representation at the level of the brainstem. Second, the amplitude-modulation rates of 37 and 81 Hz should elicit ASSRs at 37 and 81 Hz, from cortical and subcortical generators respectively. Third, passive auditory stimulation with an ISI of 500 msec should evoke the obligatory N1 and P2 components. Fourth, the infrequent transition in carrier frequency from 500 to 600 Hz should elicit the MMN, and as the carrier frequencies are easily discriminated by normal-hearing adults (Wier et al., 1977), the infrequent transition should also elicit the P3a.

This experiment intends, first, to demonstrate the viability of the SEAP method as a means of concurrently eliciting all aforementioned AEP components and, second, to collect normative data regarding how the subcortical AEP components elicited by SEAP (i.e. 81 Hz ASSR and FFR) are related to cortical components (i.e. N1, P2, MMN, P3a, and 40 Hz ASSR) within individuals during passive exposure. We expect the morphology of the subcortical FFR to predict the morphology of cortical components (e.g. 37 Hz ASSR, N1, P2), as the generators of these AEPs rely on the acoustic information being relayed forward from IC. Further, the relative onset of steady-state components (FFR and 37/81 Hz ASSRs) may be correlated across listeners in part because these components may share overlapping generators and thus be similarly affected by individual differences in the conduction velocity and response properties of neurons along the ascending auditory pathway.

2. Material and methods

2.1. Subjects

A total of 26 adult undergraduate subjects (mean 19.26 ± 1.76 years; 9 male) were recruited from the McMaster Undergraduate Psychology subject pool. After obtaining informed consent, subjects were asked to complete a brief hearing history questionnaire. All subjects self-reported to have normal hearing at the time of the experiment. Participation was remunerated in partial course credit. The research protocol was approved by the McMaster Research Ethics Board in accordance with World Medical Association Declaration of Helsinki.

2.2. Stimuli

Stimuli were created by amplitude modulating pure-tone carriers at the sum of 37 and 81 Hz to a depth of 100% (Fig. 1) according to Eq. (1):

$$y(t) = \sin(2\pi f_{carrier} t) \times ([\sin(2\pi f_{AM1} t) + \sin(2\pi f_{AM2} t)] + 1) \quad (1)$$

Modulation rates of 37 and 81 Hz were chosen so as to be non-harmonically related but close to the modulation rates evoking maximum amplitude ASSRs (i.e., 40 and 80 Hz) without creating additional modulation of the carrier signal at f_2-f_1 and allowing for later response extraction and analysis in the frequency domain. Stimuli were generated online using a Tucker-Davis Technologies (TDT) RP2.1 Enhanced Real-time Processor controlled by TDT RPvdsEX (v.5.4) software. TDT software ran on a Compaq Evo D51C (Intel P4 @ 2.4 Ghz, 1 GB RAM, Windows XP x86 SP2) and controlled the TDT RP2.1 via USB interface. Signal output from the TDT RP2.1 was routed through a TDT P5A Programmable Attenuator set at 23.9 dB to produce a stimulus presentation of level of 83 dB SPL (70 dB nHL; determined as the threshold measured in a different group of subjects). Attenuator output was passed to a TDT HB7 Headphone Driver (0 dB gain) which drove a single right-channel Etymotic ER-3A (10 Ohm) ear-insert transducer. Presentation levels were calibrated using a Bruël & Kjær Artificial Ear (Type 4152) connected to a Bruël & Kjær 2260 Investigator sound level meter (SLM).

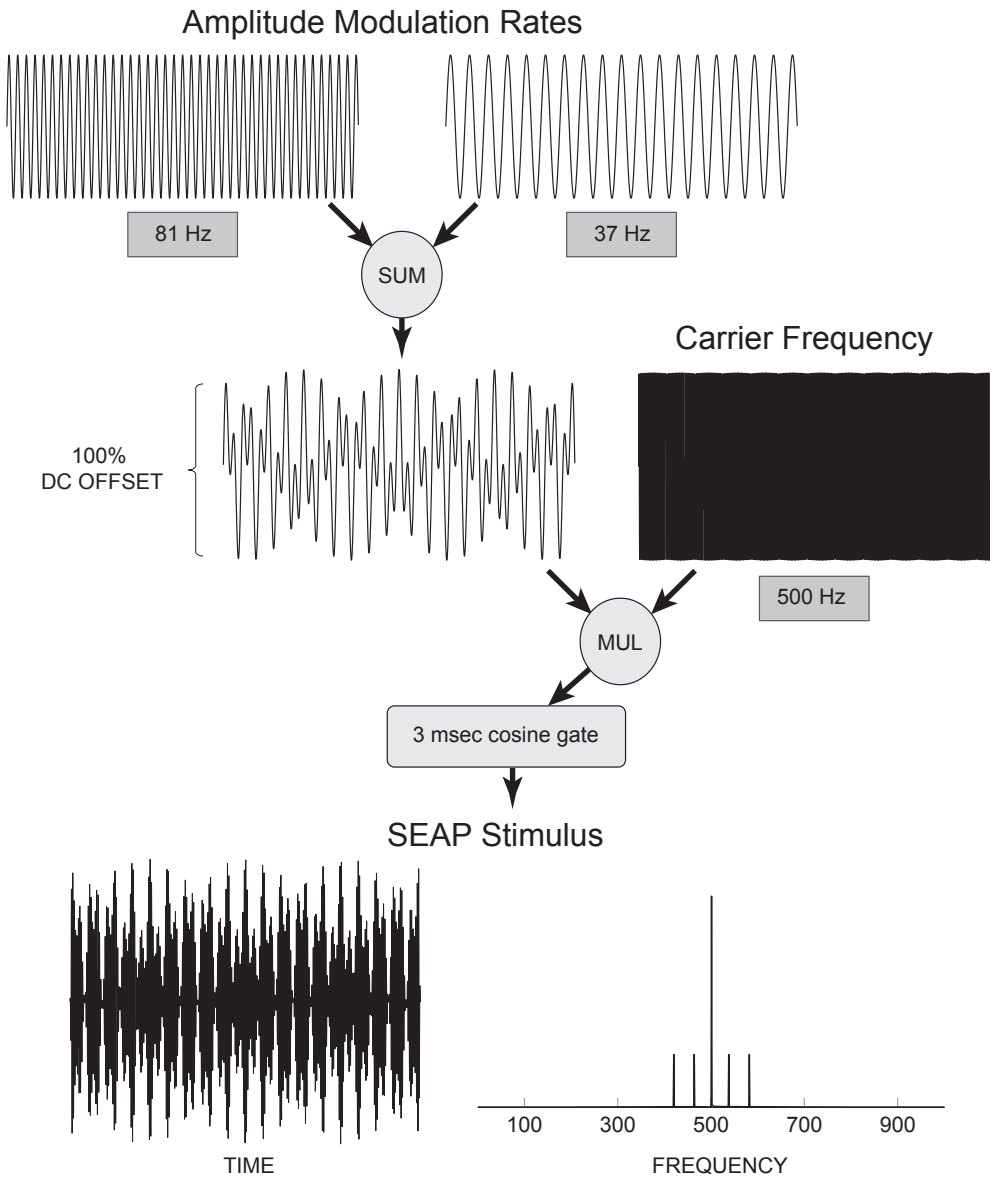

Fig. 1. Schematic representation of the SEAP stimulus generation process. Two amplitude modulation rates are chosen near 40 and 80 Hz such that they do not share a harmonic relationship. The amplitude modulation waves are summed and DC-offset by 100%. A carrier frequency (represented here by 500 Hz) is then multiplied by the summed complex modulation wave. Stimulus onset and offset are gated by a 3 msec cosine gate. The resultant stimulus is depicted in the time (bottom left) and frequency (1–1000 Hz; bottom right) domain.

To prevent electromagnetic contamination of the EEG data, the ER-3A transducer was kept outside of the sound-attenuated testing chamber. Sound was delivered to each subject through a 292 cm length of black flexible polyvinyl chloride tubing (6 mm inside-diameter) which was coupled to the stock 27.6 cm length of tubing shipped with the ER-3A unit (1.93 mm inside-diameter). Inside the testing chamber, the flexible polyvinyl chloride tube terminated in a 13 mm disposable adult foam ear-insert tip (ERI-14A; 1.93 mm inside-diameter) which was seated in the subject's right-ear canal for stimulus delivery. The entire length of the tube assembly was 320.9 cm, resulting in a theoretical delay of approximately 9.43 msec (assuming speed of sound = 340.29 m/s at sea level). Separate artifact-testing sessions were conducted weekly over the course of the experiment to ensure no stimulus artifact was contaminating the EEG recordings. In these sessions the foam tip of the stimulus tube was clamped shut and attached to the collar of a lab member. We then recorded EEG following the experimental paradigm described below. No energy was found at the stimulus frequency in the averaged EEG responses from any of these artifact-testing sessions.

A Digital Room Correction (DRC) algorithm (http://drc-fir.sourceforge.net/) was used to correct the frequency response of the modified tube assembly. The DRC algorithm produced a 1000 tap finite impulse response (FIR) filter which was applied online via TDT RPvdsEX software to correct the distribution of spectral energy for all sound output. Analysis of the impulse response generated by

the filtered output revealed nearly uniform energy (±3 dB) in the frequency domain from 20 to 4000 Hz.

A stimulus delay of 44.6 msec was measured as the time between the Transistor-transistor Logic (TTL) pulse in the EEG trace and the time of arrival for sound at the ear insert. Sound at the ear-insert was measured using a Bruël & Kjær Artificial Ear (Type 4152) connected to a Bruël & Kjær 2260 Investigator SLM. The line level output of the SLM was recorded through a bipolar channel on the SynAmps RT amplifier. All subsequent measures of component latency, as well as markers of stimulus onset, have been adjusted to reflect this delay.

2.3. Recording paradigm

During the experiment, subjects sat on a comfortable chair in a sound-attenuating booth. To maintain subject arousal, a silent DVD movie (subtitled) was displayed on a computer monitor positioned at 1 m directly in front of the chair. Subjects were instructed to remain as still as possible and focus their attention on the movie.

The experimental session consisted of a single block of 2400 trials. Trials were defined by the presentation of a stimulus (512 msec duration; 3 msec rise/fall cosine gate; fixed polarity) followed by a 500 msec silent inter-stimulus interval. The pure-tone carrier of the stimulus was set to 500 Hz for 85% of trials (standard trials). To elicit an auditory mismatch response, the frequency of the pure-tone carrier was changed to 600 Hz on 15% of trials (deviant trials). Deviant trials were interspersed pseudo-randomly into the stimulus train with the restriction that any deviant trial be separated by at least 2 standard trials (Picton et al., 2000). Standard trials immediately following deviants were eliminated from further analysis as they physically differed from the preceding stimulus. The recording block lasted approximately 40.5 min and the total experimental session, including subject orientation, electrode placement, and debriefing lasted fewer than 60 min. This paradigm collected a total of 2070 FFR trials, 2070 ASSR trials, 1740 N1/P2/MMN standard trials, and 330 MMN/P3a deviant trials per subject, prior to artifact rejection.

We collected EEG data using a Compumedics Neuroscan SynAmps RT amplifier (Model: 9032) and Compumedics SCAN 4.5 Acquire software running on an Intel PC (Intel Core i5 @ 3.33 GHz, 4 GB RAM, Windows 7 x64). The amplifier sampled voltage from the electrodes at a rate of 20,000 Hz using a 24-bit A/D converter, operating in a range of ±200 mV with a least significant bit (LSB) resolution of 23.84 nV (0.400 V/2^{24}) in DC-mode. Stimulus onset was denoted by a TTL pulse sent to the SynAmps RT amplifier from the TDT RP.2.1. Three Ag/AgCl sintered electrodes were filled with a conductive gel (Signa Gel) and attached to subjects via double-sided tape washers. Electrode placement followed the vertical montage used in auditory brainstem recording. A ground electrode was applied to the center of the forehead, a reference electrode to the back of the right earlobe (ipsilateral to stimulus delivery), and a recording electrode (Cz) to the vertex of the skull. The vertex was defined as the cranial intersection of the midway point between the ear canals and the midway point between the bridge of the nose and the inion. The recording electrode was connected to a bipolar channel on the SynAmps RT headbox and measured against the reference channel. This montage is optimal for recording evoked responses of both subcortical and cortical origin (Bidelman, 2015b; Musacchia et al., 2008). Recordings were subject to a hardware band-pass filter of 0.5–3000 Hz and a software notch filter at 60 Hz. Electrode impedance of all subjects was kept below 50 kΩs. Four subjects were excluded from further analysis for failing to maintain electrode impedance below 50 kΩ during the duration of the recording session; the mean impedance for the remaining sample was 25.20 ± 16.27 kΩs.

2.4. Data analysis

Recorded data were segmented into epochs between −94.6 and 655.4 msec, relative to stimulus onset, using BESA software (v.5.1.8). Baseline correction was applied by subtracting the mean of the pre-stimulus window from each epoch. Prior to artifact rejection, the standard and deviant response data were band-pass filtered between 0.5 and 1000 Hz (12 dB/octave; zero-phase). Epochs were rejected through BESA's artifact rejection tool if they contained activity that exceeded ±80 μV. Accepted trials were averaged according to trial type (standard or deviant) before being transferred to MATLAB R2009a (v.7.8.0.347) for further analysis.

Discrete Fourier transforms (DFTs) of the standard-evoked sustained AEPs (i.e. 37 and 81 Hz ASSRs, 500 Hz FFR) were calculated on a portion of the response ranging from 50 to 450 msec post stimulus onset. A spectral resolution of 1 Hz was interpolated by zero-padding the extracted portion of the response epoch up to 20,000 samples. Amplitudes corresponding to 500 Hz (FFR) as well as 37 and 81 Hz (ASSRs) were extracted from the DFTs of standard-evoked responses. Amplitude values for each component, as well as 40 neighboring non-response frequency bins (20 higher and 20 lower), were extracted from each subject's standard DFT data and converted into power for *F*-test verification as described in Zurek (1992). Significance of the *F* ratio was then evaluated against critical values of *F* with 2 and 80 degrees of freedom (Zurek, 1992). This test revealed significant sustained components in the standard-evoked AEPs of all but 2 subjects. Visual inspection confirmed that both subjects were missing a peak in their response power spectra at 37 Hz. One of the two subjects was also missing a peak at 81 Hz and so their data eliminated from further analysis for failing both the *F* test and visual inspection at 2 out of 3 ASSR components. Therefore, the final sample consisted of 21 subjects (mean 19.44 ± 1.93 years; 6 male). The actual sample used in each statistical measure consisted of some subset of these 21 subjects which also survived outlier elimination in each morphological category, where outliers were defined as values which fell more than 1.5 times the interquartile range above the third quartile or below the first quartile. Sustained AEP analysis was limited to standard-evoked AEPs because the greater trial count compared to deviants allowed for more reliable signal detection using the *F*-test method.

Unwrapped phase values were also extracted for the 37 and 81 Hz ASSRs. Phase unwrapping makes use of an algorithm to correct the radian phase angles in a vector by adding multiple of $\pm 2\pi$ when absolute jumps between consecutive elements of the vector are greater than or equal to π radians. In this way the instantaneous phase represented by the complex-valued DFT was made continuous allowing for calculation of phase delay as described in John and Picton (2000). In determining phase delay from unwrapped phase values, first, the measured phase was advanced by 90° to reflect the difference between the DFT phase, computed as cosine, and the phase of the stimulus, which was amplitude modulated with sine functions. Second, the adjusted phase was subtracted from 360° to represent the delay between measured phase and the leading stimulus phase (i.e. phase delay grows larger as separation increases). In order to maintain phase values between 0 and 360°, values below or above this range were adjusted by adding or subtracting 360°, respectively. Means and standard deviations for phase delay data were computed using CircStat, a circular statistics toolbox for MATLAB (Berens, 2009). The Rayleigh test was also used to measure the degree to which phase data polarized for each ASSR component in our sample of listeners. This analysis uses the length of the mean resultant vector of phase angles to test the null hypothesis that data are uniformly distributed about the unit circle (Mardia and Jupp, 2009). Significant

polarization would suggest oscillatory activity at 37 and 81 Hz did indeed phase-locked to the amplitude modulation rates of the evoking stimulus.

Phase delays were not computed for the 500 Hz FFR because the circular nature of these measures makes it difficult to interpret correlations between phases of high frequency signals and those of low frequency signals such as the 37 and 81 Hz ASSRs. The phase-locking capacity of neurons contributing to the FFR was instead assessed by cross-correlating the FFR (standard-evoked response filtered around 500 Hz) with the stimulus waveforms as recorded at the ear-insert (see **2.2 Stimulus**). Standard-evoked AEPs were band-pass filtered using Chebyshev Type II infinite impulse response filters (IIR) (Table 1). Filtering was applied in the forward and reverse direction to ensure zero phase distortion. The latency of each subject's FFR was inferred from the time shift at the maximum peak of the cross-correlation function.

To assess transient AEPs, standard and deviant responses from all subjects were forward-reverse band-pass filtered between 2 and 20 Hz using a Chebyshev Type II IIR filter (Table 1). This filter was used to remove any interfering low-frequency noise as well as energy contributed from the ASSR components. Amplitude and latency measures of the N1 and P2 components were extracted from the filtered standard responses of each subject. The peak of the N1 component was defined as the minimum peak value between 80 and 150 msec post stimulus onset. The peak of the P2 component was defined as the maximum peak value between 120 and 300 msec post stimulus onset. Difference waves were calculated by subtracting the filtered standard response from the filtered deviant response (Picton et al., 2000). The grand mean of all averaged difference waves was tested against zero at each time point using a single sample *t*-test (two-tailed, $\alpha = 0.05$, Bonferroni corrected). The MMN was defined as the largest negative peak in the difference wave occurring between 115 and 200 msec post stimulus onset where the single sample *t*-test indicated a significant negative deviation from zero (Fig. 2). Amplitude and latency values of the MMN were recorded for later statistical analyses. Similarly, amplitude and latency measures of the P3a component were extracted from the difference waves. The peak of the P3a component was defined as the maximum peak value between 225 and 295 msec post stimulus onset where the single sample *t*-test indicated a significant positive deviation from zero (Fig. 2). All peaks were selected using a peak picking algorithm in MATLAB and confirmed with visual inspection (Mathworks File Exchange: pickpeaks.m). Grand averages of the standard, deviant, and difference AEP traces were computed by averaging each response type across all participants.

Correlation analyses (2-tailed, $\alpha = 0.05$) were conducted in IBM's SPSS software (v.19.0.0) to examine relationships among the morphological features of the SEAP-evoked components. The analyses divided morphological features into timing (latency and phase delay), strength (transient peak and DFT amplitude), and fidelity (FFR-to-stimulus cross-correlation coefficient) information. Pairwise exclusion was applied to cases where data values were missing due to outlier elimination. Normality of the data was verified using the Shapiro-Wilk test ($\alpha = 0.05$). The significance of correlation coefficients computed on data not meeting normality assumptions was assessed using Spearman's ρ; otherwise, all correlations were assessed using Pearson's *r*. The 95% confidence interval (CI) of each correlation coefficient was estimated by bootstrap sampling the data 1000 times with replacement. Only those correlations whose bootstrapped confidence intervals did not contain zero were considered significant.

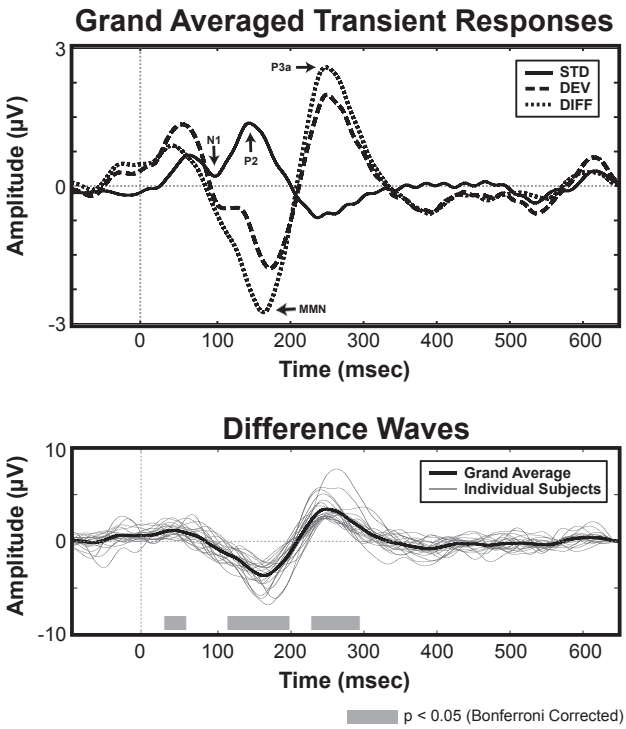

Fig. 2. TOP: Grand averaged (N = 21) transient responses elicited by standard (solid trace) and deviant (dashed trace) SEAP stimuli. The difference wave (standard response subtracted from deviant response) is shown in the dotted trace. Labels identify transient component peaks in the grand averaged waves. BOTTOM: Differences waves from individual subjects are plotted in light grey with the resultant grand average plotted in black. The grand mean of all averaged difference waves was tested against zero at each time point using a single sample *t*-test (two-tailed, $\alpha = 0.05$, Bonferroni corrected). Grey bars indicate significant deflections from zero.

Relationships in response timing and strength were measured by separately correlating timing and strength features. In order to assess whether stimulus fidelity at the level of the IC predicts response morphology at higher levels of the auditory pathway, FFR-to-stimulus cross-correlation coefficients were correlated against peak amplitude and latency values of the transient components and the DFT amplitude of the 37 Hz ASSR.

3. Results

3.1. Transient components

The grand averaged standard, deviant, and difference transient AEP waves elicited by the SEAP method are presented in Fig. 2.

Table 1
Summary of Chebyshev Type II band-pass filters.

AEP	Low-stop, Pass-band, High-stop (Hz)	Low-stop, Pass-band, High-stop (dB)
37 Hz ASSR	3, 25–55, 200	−20, 1, −30
81 Hz ASSR	40, 70–92, 190	−20, 1, −30
500 Hz FFR	200, 400–600, 800	−20, 1, −30
Transients	0.5, 2–20, 60	−20, 1, −20

Average peak amplitude and latency data for the MMN as well as the N1, P2, and P3a components are summarized in Table 2. The morphology of the MMN response is typical of MMN components elicited by pure tone deviants (Näätänen et al., 2007). Similarly, the average N1-P2 peak-to-peak amplitude (1.88 ± 1.22 μV, N = 20) corresponds well with values established in the literature (e.g. Tremblay et al., 2001) as does the P3a peak amplitude (e.g. Horváth et al., 2008), suggesting that presentation parameters used in the SEAP method are effective for eliciting these transient AEPs.

3.2. Sustained components

Time and frequency domain representations of the grand averaged sustained AEPs (ASSRs/FFRs), as evoked by standard stimulation, are shown in Fig. 3. DFT amplitudes and phase delays of the sustained components as well as stimulus-response cross-correlation coefficients and latency measures for the FFR are summarized in Table 3. The DFT amplitudes of 37 and 81 Hz ASSR components are in agreement with previously published figures (Bosnyak et al., 2007; D'haenens et al., 2008) as is the DFT amplitude of the 500 Hz FFR (Skoe and Kraus, 2010a). Polar plots of the phase delay of 37 and 81 Hz ASSR components are shown in Fig. 4. Combined with the significant results of Rayleigh's tests, these figures illustrate that the observed phase data are non-uniformly distributed around the unit circle, suggesting that neural activity is phase-locked to the amplitude modulation rates of the evoking stimulus.

3.3. Correlations

Analysis of timing information from the standard-evoked AEP components revealed significant positive correlations between: (1) latency of the 500 Hz FFR and phase delay of the 37 Hz ASSR, and (2) phase delays of the 37 and 81 Hz ASSRs (Fig. 5). Thus, the standard-evoked data suggest that the relative onset of 37 Hz ASSR activity is affected by the neural processes reflected in the 81 Hz ASSR and the FFR at 500 Hz, albeit through different mechanisms as the 81 Hz ASSR and FFR were not themselves correlated in time.

Analysis of steady-state spectral amplitude revealed a significant positive correlation between the standard-evoked 500 Hz FFR and 81 Hz ASSR (Fig. 6). This correlation might reflect proximal or overlapping generators in subcortex. Cross-correlation of the entire FFR signal with the eliciting stimulus waveform produced coefficients that significantly negatively correlated with N1 Latency (Fig. 7), which suggests that greater stimulus fidelity at the level of the IC reduced the time required for N1 generation. There were no other significant correlations among response strength data, nor did other morphological features of the remaining transient or sustained AEPs significantly correlate with FFR signal fidelity.

4. Discussion

4.1. General

To our knowledge, SEAP is the first stimulation method to simultaneously record cortical N1, P2, MMN, P3a, 40 Hz ASSR as well as subcortical FFR and 80 Hz ASSR components from normal-hearing adults. Relative to separate recordings (Bidelman et al., 2014a, 2014b; Bidelman and Alain, 2015; Krishnan et al., 2012) or clustered presentation approaches (Bidelman, 2015b), simultaneous measurement has the advantage of controlling for between-subject and between-session variance which might otherwise obfuscate relationships among AEP component morphologies. In this way, the SEAP method offers a new way to study how subcortical and cortical auditory processing stages interact in different populations of listeners as well as under different task demands or in response to different listening conditions.

The subcortical mammalian auditory system is uniquely complicated relative to other sensory systems, such as vision or somatosensation. As AEPs represent the aggregate activity of many neuron types from the many nuclei of the auditory system in response to repeated acoustic stimulation, it is impossible to know precisely which nuclei or cell types contribute to each AEP or measure their relative contribution. In the discussion that follows, we accept the most widely purported generator sites for each AEP as discussed in this paper's introduction, and adopt a largely anatomically- and physiologically-derived interpretation. However, as our data reflect the activity recorded from a single channel, all inferences made about the relationship between cortical and subcortical generators are based only on the waveform of the signal and thus remain speculative. In the future, multi-channel recordings might be useful in further isolating the source activity of each AEP component in order to make more confident assertions about the dynamics of auditory processing along the ascending auditory hierarchy.

4.2. Correlations between the timing of subcortical sustained components and the phase of cortical 40 Hz ASSR

Using SEAP, we found that the timing of neural activity in primary auditory cortex is correlated with the timing of neural activity of at least two subcortical generators. Specifically, during passive listening, the phase delay of the cortical 40 Hz ASSR was related to both the phase delay of the subcortical 80 Hz ASSR as well as the latency of the FFR at 500 Hz. However, the onsets of these two subcortical AEPs were not related to one another, so they appear to contribute independent input to the 40 Hz ASSR. Current models of the 40 Hz ASSR consider the signal to reflect the combined activity of a peripherally-driven envelope-following mechanism and a centrally-driven oscillatory mechanism (Draganova et al., 2008). One possibility is that the 80 Hz ASSR contributes mainly to the envelope-following mechanism and the FFR to the oscillatory mechanism.

Common subcortical sources of envelope-following activity might partly explain the correlation in timing between 40 and 80 Hz ASSR. Envelope information is first extracted through a demodulation process related to the non-linearity of hair cells in the cochlea (Regan and Regan, 1988). Therefore, the envelope-following activity of auditory nerve can be preserved in either subcortical or cortical sources insofar as neurons at these sources are capable of phase-locking to the envelope periodicity (Lins et al., 1995). As one ascends the auditory pathway fewer neurons are able to follow higher modulation rates and the limits of observable phase-locking decrease from about 1 to 2 kHz at the auditory nerve to less than 70 Hz in cortex (for a review see: Joris et al., 2004). Dipole solutions for human ASSR data reflect this phase-locking gradient. Sources of the 40 Hz ASSR fit to both cortical and subcortical dipoles, whereas the largest source of the 80 Hz ASSR fits to brainstem generators with minimal contribution from cortical dipoles (Herdman et al., 2002). Intracellular recordings in animal models suggest cochlear nucleus (CN) as the primary subcortical source of scalp-recorded 80 Hz ASSR activity as neurons

Table 2
Summary of peak amplitude and latency data from transient AEPs.

Transient AEP	N	Peak Amplitude (μV)	Peak Latency (msec)
MMN	21	−3.76 ± 1.23	166.02 ± 12.13
N1	20	0.05 ± 0.83	106.09 ± 11.82
P2	21	1.98 ± 0.68	153.40 ± 12.31
P3a	21	3.68 ± 1.36	258.81 ± 13.71

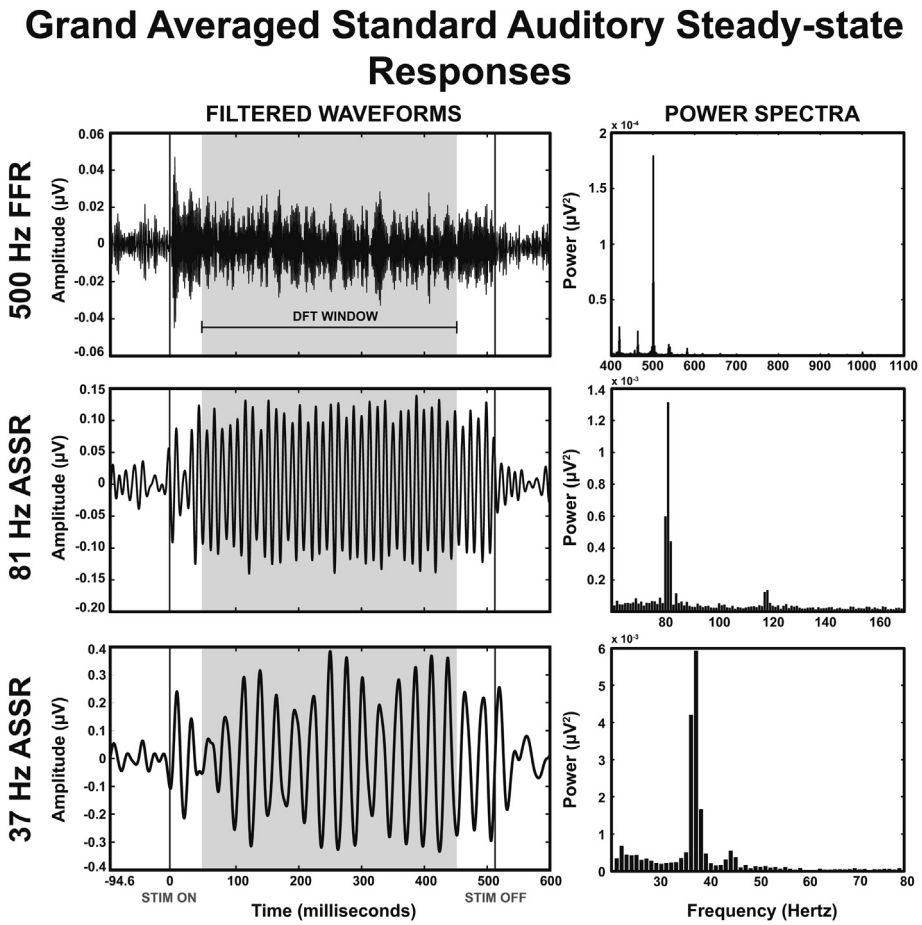

Fig. 3. Grand averaged (N = 21) auditory steady-state (ASSR\FFR) responses elicited by standard SEAP stimuli. The left column displays the grand averaged response in the time-domain as filtered to visualize the 500 Hz FFR (top), 81 Hz ASSR (middle), and 37 Hz ASSR (bottom). Vertical lines at 0 and 512 msec denote stimulus onset and offset, respectively. Light grey blocks in the time-domain indicate the window (50–450 msec post stimulus-onset) over which the DFT was measured. The right column displays the power spectrum of each response as measured from the DFT window.

Table 3
Summary of steady-state AEP morphology.

Sustained AEP	N	Amplitude ($\mu V \cdot 10^{-2}$)	Phase Delay
37 Hz ASSR	21	7.10 ± 3.07	234.61 ± 27.00
81 Hz ASSR	21	3.16 ± 1.82	71.85 ± 31.97
500 Hz FFR	21	1.14 ± 0.71	64.15 ± 67.57
		X-Corr. Coefficient	**X-Corr. Latency**
500 Hz FFR	18	0.67 ± 0.19	4.23 ± 2.14

there respond best to amplitude-modulation rates above 80 Hz (Frisina et al., 1990; Suzuki, 2000). CN is the terminus of Type I auditory nerve fibers (ANFs), which carry information about inner hair cell activity via bipolar spiral ganglion cells. The onset of activity in ANFs is, among other factors, affected by the structure (e.g. ear canal and basilar membrane length) and function (e.g. cochlear filter delay) of peripheral hearing organs. The phase delay measured from both 40 and 80 Hz ASSRs is demonstrably sensitive to variation in the timing of acoustic transduction and, for example, increases systematically with increasing carrier frequency as a result of the frequency-dependent travelling wave mechanics of the basilar membrane (Greenberg et al., 1998; John and Picton, 2000; Ross et al., 2000). To the extent that 40 Hz ASSR also reflects subcortical envelope-following activity, the onset of both 40 and 80 Hz ASSR components could be similarly affected by individual differences in the physiology and overall health of peripheral auditory structures or neural conductance velocity across our sample of listeners.

On the other hand, the correlation we observe between the timing of the 40 Hz ASSR and the FFR might be more likely reflect neural synchrony between activity in IC and the central oscillatory mechanism of the 40 Hz ASSR rather than an envelope-following mechanism. Cortical and thalamic sources of the 40 Hz ASSR are thought to support local neural oscillations via interactions between excitatory and inhibitory connections within a thalamocortical loop. Neural network models suggest such loops resonate maximally to periodic sensory input at frequencies close to 40 Hz (Llinás and Ribary, 2001). Neurons in the central nucleus of the IC constitute the primary lemniscal input to the ventral division of the medial geniculate body of the thalamus (Malmierca, 2015). Extracellular recordings in rabbit models find neurons in IC respond best to modulation rates between 20 and 40 Hz (Batra et al., 1989), implicating IC as a major subcortical contributor to 40 Hz ASSR. It follows, then, that the onset of activity at IC, as indexed by FFR latency, might strongly influence the rate at which these thalamocortical oscillations enter into a resonant state at 40 Hz.

Further, the timing of activity at IC appears to be more strongly related to the activity of these thalamocortical circuits than to ascending input as we did not observe a timing correlation between the FFR and the 80 Hz ASSR. It is possible that coordinated timing between the subcortical 80 Hz ASSR and FFR components might

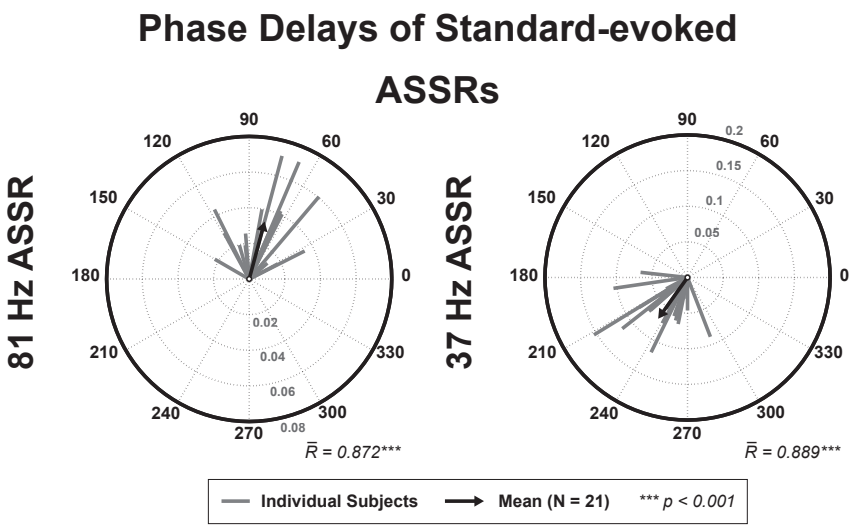

Fig. 4. Polar plots of the phase delay for each ASSR component elicited by standard presentations of the SEAP stimulus. Grey vectors represent the phase delay of individual subject responses. Black arrowhead vectors represent the average phase delay for each component (N = 21). Amplitudes are represented by vector length. The mean resultant vector length ($\bar{R}$) of the phase angles with uniform amplitude was significant for both 37 and 81 Hz ASSR components ($p < 0.001$).

have been obscured by individual differences in neuroanatomy and neural conductance velocity. Assuming the primary generator of 80 Hz ASSR is indeed CN, then a greater number of synaptic relays separate 80 Hz ASSR activity from FFR activity at IC compared to those that separate FFR activity from thalamocortical generators of the 40 Hz ASSR. On the other hand, the correlation between 80 Hz ASSR and FFR amplitudes suggest that these components originate from proximal sources or even partially overlapping sources.

Another possibility is that the latency of processing at IC might be affected by descending corticofugal projections in a way that does not affect the envelope-following mechanism which generates 80 Hz ASSR. Indeed, reversible ablation of auditory cortex in rat models has been shown to prolong the latency of evoked responses generated in IC (Nwabueze-Ogbo et al., 2002). Moreover, sleep (Aoyagi et al., 1993; Cohen et al., 1991) and general anesthetic (e.g. propofol; Plourde et al., 2008), both of which result in hyperpolarization of thalamocortical neurons and therefore reduced information flow to cortex, have been found to attenuate both subcortical and cortical sources of the 40 Hz ASSR equally, but have no effect on the 80 Hz ASSR. Moreover, the amplitude of scalp-recorded low-frequency ASSR (around 40 Hz) in rabbit is diminished by administration of pentobarbital anesthesia and by potassium chloride-induced cortical depression. Conversely, low-frequency ASSR is enhanced through arousal (cocaine administration and tactile stimulation). No such modification is observed in the ASSR elicited by higher (e.g. > 80 Hz) modulation rates (Kuwada et al., 2002). Presumably, sleep should not affect subcortical envelope-following responses, though whether sleeping subjects show enhanced timing correlations between the 40 and 80 Hz ASSR components and diminished timing correlations between 40 Hz ASSR and FFR remains an open question for future research.

One significant limitation inherent in using fixed polarity presentation to measure FFR is that one cannot rule out possible peripheral contributions from auditory nerve (Bidelman, 2015a). Indeed some measures of FFR latency are unrealistically short (<2 msec) for sources in upper brainstem. However, if our FFR signal mainly reflects activity at AN then it is peculiar that we did not observe a strong timing relationship between FFR latency and the phase of the 80 Hz ASSR whose generators are largely limited to lower brainstem (Herdman et al., 2002). As we did not limit the lag of the largest stimulus-to-FFR cross-correlation coefficient, it is possible that the shortest of these FFR latencies reflect diminishing fidelity of the FFR signal over time in certain individuals. Alternatively, our method of recording the stimulus waveform from the line level output of sound level meter into the bipolar channels of our EEG amplifier might have introduced delay that was unaccounted for when measuring the lag of maximum cross-correlation coefficient. Further, the average amplitudes of many FFR components at 500 Hz and the 80 Hz ASSR fall below the technical resolution of the EEG system in DC-mode (~24 nV). These data are thus extrapolated from averaging and any correlations involving the morphology of these components are, in fact, between approximated values. Future study might use AC-coupled amplifier input to improve the resolution of the system to 3 nV/bit at the cost of attenuating/distorting low-frequency information in the signal.

4.3. Subcortical acoustic feature representation and cortical processing

Our data further suggest that the fidelity of acoustic feature representation at the level of subcortex is related to the time required for acoustic feature integration at the cortical level. Specifically, we found the strength of the cross-correlation between the FFR signal and the acoustic stimulus to be negatively associated with the latency of the N1 component. This result adds to the distinction between 40 Hz ASSR and N1 by demonstrating that the underlying generators of these components differ in their interaction with auditory-evoked activity from subcortical generators. Though both the 40 Hz ASSR and the N1 are often localized to sources in Heschl's gyrus, these components reflect distinct neural networks which differ in both their tuning properties (Ross et al., 2003) and specific dipole solutions (Draganova et al., 2008). Sources of the 40 Hz ASSR reportedly lie deep in Heschl's gyrus bilaterally (Draganova et al., 2002; Engelien et al., 2000; Ross et al., 2002), in regions widely accepted as the location of primary ACs (Da Costa et al., 2011; Penhune et al., 1996). The 40 Hz ASSR also implicates source activity from a midbrain or subcortical structure likely around thalamus or IC (Herdman et al., 2002). In contrast, sources of the N1 are exclusively cortical and localized to the lateral part of Heschl's gyrus and the planum temporale (Godey et al., 2001; Pantev et al., 1995). As such, 40 Hz ASSR probably reflects the earliest activation of primary AC via thalamocortical circuits,

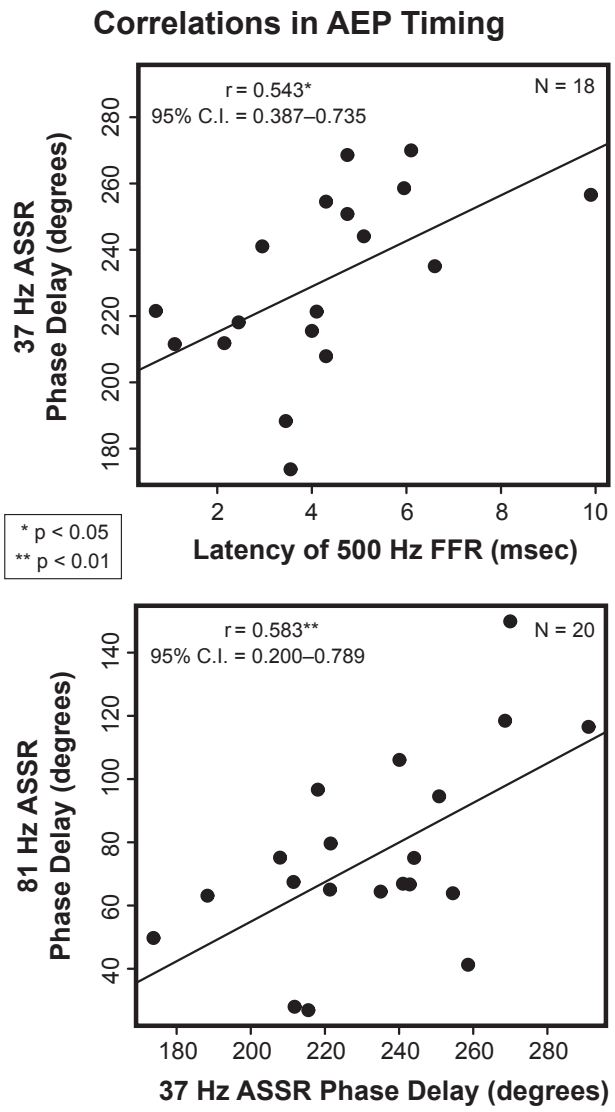

Fig. 5. Scatterplot of significant correlations (two-tailed Pearson's Correlation Analysis, $p < 0.05$) between timing information in the SEAP components as elicited by presentation of the standard stimulus. –**TOP**: latency of the standard 500 Hz FFR component (as measured through cross-correlation with the stimulus waveform) and phase delay of the 37 Hz ASSR component. **BOTTOM**: phase delays of the 37 and 81 Hz ASSR components.

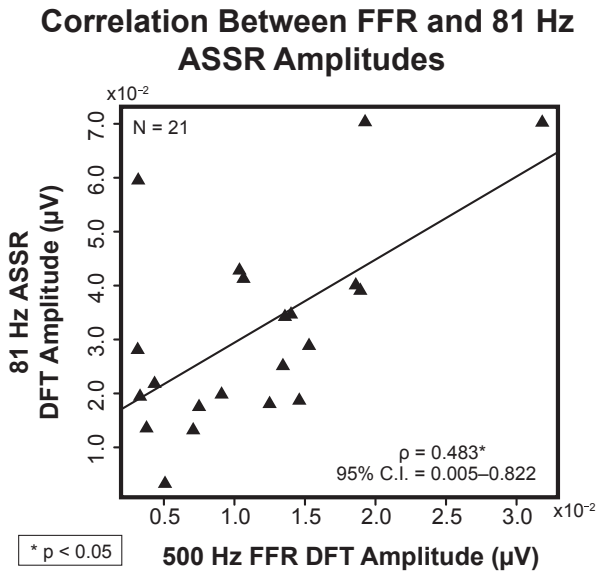

Fig. 6. Scatterplot of a significant correlation (two-tailed Spearman's Correlation Analysis, $p < 0.05$) between amplitude information in the 500 Hz FFR and the 81 Hz ASSR as elicited by frequently-presented (standard) stimuli.

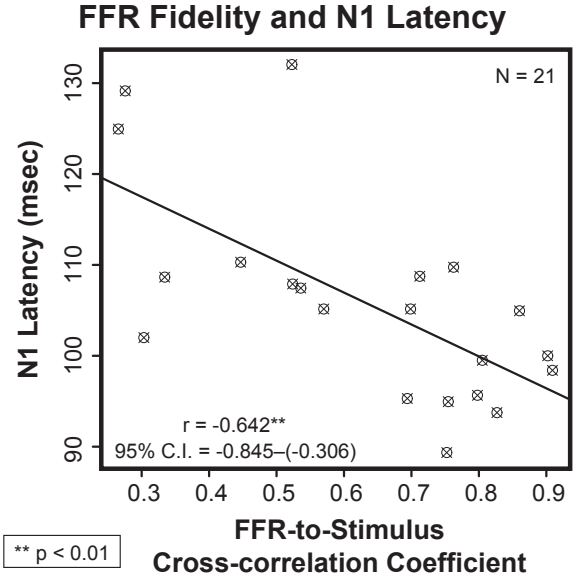

Fig. 7. Scatterplot of the significant correlation ($p < 0.01$) between the FFR-stimulus cross-correlation coefficient (standard response) and the latency of the transient N1 component.

whereas N1 involves more synapses spread across primary and secondary AC (Eggermont and Ponton, 2003; Godey et al., 2001).

Unlike the FFR, the N1 is not sensitive to pitch salience per se (Krishnan et al., 2012; Winkler et al., 1997), though it is thought to reflect an indexing of exogenous stimulus features at the level of cortex (Alain et al., 2007; Bidelman et al., 2013). Given that auditory information must first be represented at subcortical nuclei before reaching cortex, it is reasonable to speculate that the quality of this subcortical representation might also impact N1 morphology. Consistent with this idea, learning disabilities involving phonological awareness, reading comprehension, and speech-in-noise discrimination are associated both with poor subcortical stimulus representation in the FFR component (Banai et al., 2005, 2009; Hornickel et al., 2009; King et al., 2002) as well as delayed N1 latency (Tonnquist-Uhlén et al., 1996). Similar changes to FFR and N1 morphology are observed in senescence and are also accompanied by speech processing deficits (Clinard and Tremblay, 2013; Tremblay et al., 2002). Consistently, auditory training improves stimulus fidelity in the FFR signal (Anderson et al., 2013; Carcagno and Plack, 2011; Song et al., 2008) and advances the onset of N1 (Bosnyak et al., 2004). Extensive auditory training (i.e. musicianship) has even been shown to offset age-related declines in speech sound processing and preserve FFR and N1 morphology in older listeners (Bidelman et al., 2014a; Bidelman and Alain, 2015; Parbery-Clark et al., 2012; Zendel and Alain, 2014).

As relatively few studies have directly compared FFR and N1 components in individual listeners, the nature of the relationship between FFR generators and early composite measures of cortical activity is still largely unclear. Musacchia et al. (2008) found the FFR spectral amplitude of a fundamental frequency component elicited

by the speech syllable “da” to strongly predict the slope of the P1-N1 complex. Moreover, the authors found this relationship to be stronger in musicians than non-musicians, and both FFR amplitude and P1-N1 slope correlated with the number of years that musicians actively engaged in musical training. Musicians also exhibited larger and earlier P1 and N1 peaks in response to the “da” stimulus relative to their non-musician counterparts. In contrast, Bidelman et al. (2014b) failed to find a difference between young adult musicians and non-musicians in either N1 amplitude or latency when evoked by vowel sounds in a categorical perception task. Additionally, the authors did not find a correlation between the morphology of the N1 and FFR components in either group. However, in older listeners, the same stimulation paradigm was found to evoke earlier N1 components in musicians relative to non-musician controls (Bidelman and Alain, 2015). Further, N1-P2 peak-to-peak amplitudes as well as FFR fundamental amplitudes were robust predictors of musicians' performance on the categorical perception task, whereas only FFR amplitude predicted non-musicians' performance suggesting that musicianship facilitated coordinated processing in subcortical and cortical generators, perhaps through enhanced corticofugal feedback. Of course, we must keep in mind that all AEPs reflect an aggregate of neural activity and several overlapping subcomponents of the N1 have been identified to respond differentially across different conditions. Differences in stimulation paradigms and stimulus features may engage cortical and subcortical processes differently. Our results, together with earlier studies, suggest that faithful encoding of stimulus features at the level of subcortex is associated with faster cortical processing.

4.4. Novelty detection along the auditory hierarchy

Contrary to our expectations, FFR fidelity did not predict the morphology of either the MMN or P3a components. However, the change used in this experiment was easily perceptible (pure tone change from 500 to 600 Hz) and so could have saturated MMN generators despite variable spectro-temporal representations at the level of IC. Other studies have shown change detection to be a property of multiple stages along ascending auditory neuraxis (for reviews see: Escera and Malmierca, 2014; Grimm et al., 2016). However, the auditory signal becomes increasingly abstracted as it ascends the auditory neuraxis (Imaizumi and Lee, 2014). The fidelity of spectro-temporal information at subcortex, then, might not strongly influence the morphology of components generated in secondary auditory cortex, particularly for stimuli that are readily discriminated. Manipulating subject attention through task-demands might also be required to engage the corticofugal circuitry required to coordinate the activity reflected in subcortical and cortical AEP morphology. We are currently using SEAP in a paradigm similar to that of Cacciaglia et al. (2015) to examine whether automatic attentional responses to occasional deviants in a stream of standards stimuli modify the relationships we observed here under passive-listening.

5. Conclusions

We demonstrate that the SEAP method can viably record several well-studied subcortical and cortical AEP components simultaneously in human adult listeners. In a passive-listening context, better stimulus fidelity at subcortical FFR generators was related to earlier onset of the cortical N1, suggesting that the spectro-temporal fidelity of ascending auditory information promotes neural synchrony and temporal integration at N1 generators. The correlation between FFR latency and 40 Hz ASSR phase delay further supports a link between neural activity at IC and early cortical processing. However, we failed to find a relationship between stimulus fidelity at FFR generators and the morphology of change-detection or attention-orienting components from secondary auditory cortices (i.e. MMN and P3a, respectively). Because a large and easily perceptible stimulus change was used, ceiling effects may have precluded seeing any such potential relationships. Future studies might use less perceptible stimulus differences to probe whether MMN elicitation in individual subjects is related to the quality of subcortical acoustic feature representation.

As this experiment only recorded AEPs evoked under passive listening conditions, we can make no assertions regarding the causality of these relationships, be they feed-forward, or top-down, or some combination thereof. Presumably, the influence of top-down mechanisms is relatively limited as this experiment presented non-biologically-relevant pure tones and did not demand a response from the listeners, but it is possible that there was some bottom-up learning during the course of the experiment (see Chandrasekaran et al., 2014 for a review of bottom-up and top-down influences on subcortical FFR). Nevertheless, concurrent measurement of activity from multiple auditory nuclei in individual subjects opens an avenue for assessing dynamic relationships between auditory processing stages in a way that is unaffected by differences in recording paradigms, or by between-subject and between-session variability. Further, true simultaneous AEP measurement permits careful examination of the temporal dynamics between subcortical and cortical AEPs as they might be affected by attention, development, and experience-dependent plastic processes. In this way, the SEAP method should prove particularly useful in delineating the influence of corticofugal projections throughout early infancy as well as in assessing the efficacy of hearing-related interventions on acoustic feature representation at the level of cortex and subcortex.

Acknowledgements

This work was supported by grants to LJT from the Natural Sciences and Engineering Research Council of Canada (RGPIN-2014-0470) and the Canadian Institutes of Health Research (MOP 42554). We thank Elaine Whiskin for technical assistance.

References

Alain, C., Snyder, J.S., He, Y., Reinke, K.S., 2007. Changes in auditory cortex parallel rapid perceptual learning. Cereb. Cortex 17, 1074–1084. http://dx.doi.org/10.1093/cercor/bhl018.

Anderson, S., White-Schwoch, T., Parbery-Clark, A., Kraus, N., 2013. Reversal of age-related neural timing delays with training. Proc. Natl. Acad. Sci. 110, 4357–4362. http://dx.doi.org/10.1073/pnas.1213555110.

Aoyagi, M., Kiren, T., Kim, Y., Suzuki, Y., Fuse, T., Koike, Y., 1993. Optimal modulation frequency for amplitude-modulation following response in young children during sleep. Hear. Res. 65, 253–261. http://dx.doi.org/10.1016/0378-5955(93)90218-P.

Atienza, M., Cantero, J.L., Stickgold, R., 2004. Posttraining sleep enhances automaticity in perceptual discrimination. J. Cogn. Neurosci. 16, 53–64. http://dx.doi.org/10.1162/089892904322755557.

Ballachanda, B.B., Moushegian, G., Stillman, R.D., 1992. Adaptation of the auditory brainstem response: effects of click intensity, polarity, and position. J. Am. Acad. Audiol. 3, 275–282.

Banai, K., Hornickel, J., Skoe, E., Nicol, T., Zecker, S., Kraus, N., 2009. Reading and subcortical auditory function. Cereb. Cortex 19, 2699–2707. http://dx.doi.org/10.1093/cercor/bhp024.

Banai, K., Nicol, T., Zecker, S.G., Kraus, N., 2005. Brainstem timing: implications for cortical processing and literacy. J. Neurosci. 25, 9850–9857. http://dx.doi.org/10.1523/JNEUROSCI.2373-05.2005.

Batra, R., Kuwada, S., Stanford, T.R., 1989. Temporal coding of envelopes and their interaural delays in the inferior colliculus of the unanesthetized rabbit. J. Neurophysiol. 61, 257–268.

Berens, P., 2009. CircStat: a MATLAB toolbox for circular statistics. J. Stat. Softw. 31, 1–21.

Bidelman, G.M., 2015a. Towards an optimal paradigm for simultaneously recording cortical and brainstem auditory evoked potentials. J. Neurosci. Methods 241, 94–100. http://dx.doi.org/10.1016/j.jneumeth.2014.12.019.

Bidelman, G.M., 2015b. Multichannel recordings of the human brainstem

frequency-following response: scalp topography, source generators, and distinctions from the transient ABR. Hear. Res. 323, 68–80. http://dx.doi.org/10.1016/j.heares.2015.01.011.
Bidelman, G.M., Alain, C., 2015. Musical training orchestrates coordinated neuroplasticity in auditory brainstem and cortex to counteract age-related declines in categorical vowel perception. J. Neurosci. 35, 1240–1249. http://dx.doi.org/10.1523/JNEUROSCI.3292-14.2015.
Bidelman, G.M., Krishnan, A., Gandour, J.T., 2011. Enhanced brainstem encoding predicts musicians' perceptual advantages with pitch. Eur. J. Neurosci. 33, 530–538. http://dx.doi.org/10.1111/j.1460-9568.2010.07527.x.
Bidelman, G.M., Moreno, S., Alain, C., 2013. Tracing the emergence of categorical speech perception in the human auditory system. NeuroImage 79, 201–212. http://dx.doi.org/10.1016/j.neuroimage.2013.04.093.
Bidelman, G.M., Villafuerte, J.W., Moreno, S., Alain, C., 2014a. Age-related changes in the subcortical–cortical encoding and categorical perception of speech. Neurobiol. Aging 35, 2526–2540. http://dx.doi.org/10.1016/j.neurobiolaging.2014.05.006.
Bidelman, G.M., Weiss, M.W., Moreno, S., Alain, C., 2014b. Coordinated plasticity in brainstem and auditory cortex contributes to enhanced categorical speech perception in musicians. Eur. J. Neurosci. 40, 2662–2673. http://dx.doi.org/10.1111/ejn.12627.
Bosnyak, D.J., Eaton, R.A., Roberts, L.E., 2004. Distributed auditory cortical representations are modified when non-musicians are trained at pitch discrimination with 40 Hz amplitude modulated tones. Cereb. Cortex 14, 1088–1099. http://dx.doi.org/10.1093/cercor/bhh068.
Bosnyak, D.J., Gander, P.E., Roberts, L.E., 2007. Does auditory discrimination training modify representations in both primary and secondary auditory cortex? Int. Congr. Ser., New Frontiers in Biomagnetism. In: Proceedings of the 15th International Conference on Biomagnetism, Vancouver, BC, Canada, August 21-25, 2006 1300, pp. 25–28. http://dx.doi.org/10.1016/j.ics.2006.12.040.
Burkard, R.F., Eggermont, J.J., Don, M. (Eds.), 2007. Auditory Evoked Potentials: Basic Principles and Clinical Application. Lippincott Williams & Wilkins, Philadelphia, PA.
Cacciaglia, R., Escera, C., Slabu, L., Grimm, S., Sanjuán, A., Ventura-Campos, N., Ávila, C., 2015. Involvement of the human midbrain and thalamus in auditory deviance detection. Neuropsychologia 68, 51–58. http://dx.doi.org/10.1016/j.neuropsychologia.2015.01.001.
Carcagno, S., Plack, C.J., 2011. Subcortical plasticity following perceptual learning in a pitch discrimination task. J. Assoc. Res. Otolaryngol. 12, 89–100. http://dx.doi.org/10.1007/s10162-010-0236-1.
Chandrasekaran, B., Kraus, N., 2010. The scalp-recorded brainstem response to speech: neural origins and plasticity. Psychophysiology 47, 236–246. http://dx.doi.org/10.1111/j.1469-8986.2009.00928.x.
Chandrasekaran, B., Skoe, E., Kraus, N., 2014. An integrative model of subcortical auditory plasticity. Brain Topogr. 27, 539–552. http://dx.doi.org/10.1007/s10548-013-0323-9.
Clinard, C.G., Tremblay, K.L., 2013. Aging degrades the neural encoding of simple and complex sounds in the human brainstem. J. Am. Acad. Audiol. 24, 590–599. http://dx.doi.org/10.3766/jaaa.24.7.7. -644.
Coffey, E.B.J., Herholz, S.C., Chepesiuk, A.M.P., Baillet, S., Zatorre, R.J., 2016. Cortical contributions to the auditory frequency-following response revealed by MEG. Nat. Commun. 7, 11070. http://dx.doi.org/10.1038/ncomms11070.
Cohen, L.T., Rickards, F.W., Clark, G.M., 1991. A comparison of steady-state evoked potentials to modulated tones in awake and sleeping humans. J. Acoust. Soc. Am. 90, 2467–2479. http://dx.doi.org/10.1121/1.402050.
Da Costa, S., van der Zwaag, W., Marques, J.P., Frackowiak, R.S.J., Clarke, S., Saenz, M., 2011. Human primary auditory cortex follows the shape of Heschl's gyrus. J. Neurosci. 31, 14067–14075. http://dx.doi.org/10.1523/JNEUROSCI.2000-11.2011.
Davis, H., Mast, T., Yoshie, N., Zerlin, S., 1966. The slow response of the human cortex to auditory stimuli: recovery process. Electroencephalogr. Clin. Neurophysiol. 21, 105–113. http://dx.doi.org/10.1016/0013-4694(66)90118-0.
D'haenens, W., Vinck, B.M., Vel, E.D., Maes, L., Bockstael, A., Keppler, H., Philips, B., Swinnen, F., Dhooge, I., 2008. Auditory steady-state responses in normal hearing adults: a test-retest reliability study. Int. J. Audiol. 47, 489–498. http://dx.doi.org/10.1080/14992020802116136.
Draganova, R., Ross, B., Borgmann, C., Pantev, C., 2002. Auditory cortical response patterns to multiple rhythms of AM sound. Ear Hear 23, 254–265.
Draganova, R., Ross, B., Wollbrink, A., Pantev, C., 2008. Cortical steady-state responses to central and peripheral auditory beats. Cereb. Cortex 18, 1193–1200. http://dx.doi.org/10.1093/cercor/bhm153.
Eggermont, J.J., 2007. Electric and magnetic fields of synchronous neural activity: peripheral and central origins of auditory evoked potentials. In: Auditory Evoked Potentials: Basic Principles and Clinical Application. Lippincott Williams & Wilkins, Baltimore.
Eggermont, J.J., Ponton, C.W., 2003. Auditory-evoked potential studies of cortical maturation in normal hearing and implanted children: correlations with changes in structure and speech perception. Acta Otolaryngol. (Stockh.) 123, 249–252. http://dx.doi.org/10.1080/0036554021000028098.
Engelien, A., Schulz, M., Ross, B., Arolt, V., Pantev, C., 2000. A combined functional in vivo measure for primary and secondary auditory cortices. Hear. Res. 148, 153–160. http://dx.doi.org/10.1016/S0378-5955(00)00148-9.
Escera, C., Malmierca, M.S., 2014. The auditory novelty system: an attempt to integrate human and animal research: the auditory novelty system. Psychophysiology 51, 111–123. http://dx.doi.org/10.1111/psyp.12156.
Frisina, R.D., Smith, R.L., Chamberlain, S.C., 1990. Encoding of amplitude modulation in the gerbil cochlear nucleus: I. A hierarchy of enhancement. Hear. Res. 44, 99–122. http://dx.doi.org/10.1016/0378-5955(90)90074-Y.
Galambos, R., Makeig, S., Talmachoff, P.J., 1981. A 40-Hz auditory potential recorded from the human scalp. Proc. Natl. Acad. Sci. 78, 2643–2647.
Gander, P.E., Bosnyak, D.J., Roberts, L.E., 2010. Acoustic experience but not attention modifies neural population phase expressed in human primary auditory cortex. Hear. Res. 269, 81–94. http://dx.doi.org/10.1016/j.heares.2010.07.001.
Godey, B., Schwartz, D., de Graaf, J.B., Chauvel, P., Liégeois-Chauvel, C., 2001. Neuromagnetic source localization of auditory evoked fields and intracerebral evoked potentials: a comparison of data in the same patients. Clin. Neurophysiol. 112, 1850–1859. http://dx.doi.org/10.1016/S1388-2457(01)00636-8.
Greenberg, S., Poeppel, D., Roberts, T., 1998. A space-time theory of pitch and timbre based on cortical expansion of the cochlear traveling wave delay. In: Palmer, A., Rees, A., Summerfield, Q., Meddis, R. (Eds.), Psychophysical and Physiological Advances in Hearing. Whurr, London, pp. 293–300.
Grimm, S., Escera, C., Nelken, I., 2016. Early indices of deviance detection in humans and animal models. Biol. Psychol 116, 23–27. http://dx.doi.org/10.1016/j.biopsycho.2015.11.017. Understanding the neurobiology of MMN and its reduction in schizophrenia.
Herdman, A.T., Lins, O., Roon, P.V., Stapells, D.R., Scherg, M., Picton, T.W., 2002. Intracerebral sources of human auditory steady-state responses. Brain Topogr. 15, 69–86. http://dx.doi.org/10.1023/A:1021470822922.
Hornickel, J., Skoe, E., Nicol, T., Zecker, S., Kraus, N., 2009. Subcortical differentiation of stop consonants relates to reading and speech-in-noise perception. Proc. Natl. Acad. Sci. U. S. A. 106, 13022–13027. http://dx.doi.org/10.1073/pnas.0901123106.
Horváth, J., Winkler, I., Bendixen, A., 2008. Do N1/MMN, P3a, and RON form a strongly coupled chain reflecting the three stages of auditory distraction? Biol. Psychol. 79, 139–147. http://dx.doi.org/10.1016/j.biopsycho.2008.04.001.
Imaizumi, K., Lee, C.C., 2014. Frequency transformation in the auditory lemniscal thalamocortical system. Front. Neural Circuits 8. http://dx.doi.org/10.3389/fncir.2014.00075.
John, M.S., Picton, T.W., 2000. Human auditory steady-state responses to amplitude-modulated tones: phase and latency measurements. Hear. Res. 141, 57–79. http://dx.doi.org/10.1016/S0378-5955(99)00209-9.
Joris, P.X., Schreiner, C.E., Rees, A., 2004. Neural processing of amplitude-modulated sounds. Physiol. Rev. 84, 541–577. http://dx.doi.org/10.1152/physrev.00029.2003.
King, C., Warrier, C.M., Hayes, E., Kraus, N., 2002. Deficits in auditory brainstem pathway encoding of speech sounds in children with learning problems. Neurosci. Lett. 319, 111–115. http://dx.doi.org/10.1016/S0304-3940(01)02556-3.
Kraus, N., Nicol, T., 2005. Brainstem origins for cortical "what" and "where" pathways in the auditory system. Trends Neurosci. 28, 176–181. http://dx.doi.org/10.1016/j.tins.2005.02.003.
Krishnan, A., 2007. Frequency-following response. In: Burkard, R.F., Eggermont, J.J., Don, M. (Eds.), Auditory Evoked Potentials: Basic Principles and Clinical Application. Lippincott Williams & Wilkins, Philadelphia, PA, pp. 313–335.
Krishnan, A., Bidelman, G.M., Gandour, J.T., 2010a. Neural representation of pitch salience in the human brainstem revealed by psychophysical and electrophysiological indices. Hear. Res. 268, 60–66. http://dx.doi.org/10.1016/j.heares.2010.04.016.
Krishnan, A., Bidelman, G.M., Smalt, C.J., Ananthakrishnan, S., Gandour, J.T., 2012. Relationship between brainstem, cortical and behavioral measures relevant to pitch salience in humans. Neuropsychologia 50, 2849–2859. http://dx.doi.org/10.1016/j.neuropsychologia.2012.08.013.
Krishnan, A., Gandour, J.T., Bidelman, G.M., 2010b. The effects of tone language experience on pitch processing in the brainstem. J. Neurolinguistics 23, 81–95. http://dx.doi.org/10.1016/j.jneuroling.2009.09.001.
Krishnan, A., Gandour, J.T., Bidelman, G.M., Swaminathan, J., 2009. Experience dependent neural representation of dynamic pitch in the brainstem. Neuroreport 20, 408–413. http://dx.doi.org/10.1097/WNR.0b013e3283263000.
Krishnan, A., Swaminathan, J., Gandour, J.T., 2008. Experience-dependent enhancement of linguistic pitch representation in the brainstem is not specific to a speech context. J. Cogn. Neurosci. 21, 1092–1105. http://dx.doi.org/10.1162/jocn.2009.21077.
Krishnan, A., Xu, Y., Gandour, J., Cariani, P., 2005. Encoding of pitch in the human brainstem is sensitive to language experience. Cogn. Brain Res. 25, 161–168. http://dx.doi.org/10.1016/j.cogbrainres.2005.05.004.
Krizman, J., Marian, V., Shook, A., Skoe, E., Kraus, N., 2012. Subcortical encoding of sound is enhanced in bilinguals and relates to executive function advantages. Proc. Natl. Acad. Sci. 109, 7877–7881. http://dx.doi.org/10.1073/pnas.1201575109.
Kuwada, S., Anderson, J.S., Batra, R., Fitzpatrick, D.C., Teissier, N., D'Angelo, W.R., 2002. Sources of the scalp-recorded amplitude-modulation following response. J. Am. Acad. Audiol. 13, 188–204.
Lins, O.G., Picton, P.E., Picton, T.W., Champagne, S.C., Durieux-Smith, A., 1995. Auditory steady-state responses to tones amplitude-modulated at 80–110 Hz. J. Acoust. Soc. Am. 97, 3051–3063. http://dx.doi.org/10.1121/1.411869.
Llinás, R., Ribary, U., 2001. Consciousness and the. Brain. Ann. N. Y. Acad. Sci. 929, 166–175. http://dx.doi.org/10.1111/j.1749-6632.2001.tb05715.x.
Luck, S.J., 2005. An Introduction to the Event-related Potential Technique. MIT Press, Cambridge.
Malmierca, M.S., 2015. Anatomy and physiology of the mammalian auditory system. In: Jaeger, D., Jung, R. (Eds.), Encyclopedia of Computational Neuroscience.

Springer New York, pp. 155–186. http://dx.doi.org/10.1007/978-1-4614-6675-8_286.
Mardia, K.V., Jupp, P.E., 2009. Directional Statistics. John Wiley & Sons.
Musacchia, G., Strait, D., Kraus, N., 2008. Relationships between behavior, brainstem and cortical encoding of seen and heard speech in musicians and non-musicians. Hear. Res. 241, 34–42. http://dx.doi.org/10.1016/j.heares.2008.04.013.
Näätänen, R., 2008. Mismatch negativity (MMN) as an index of central auditory system plasticity. Int. J. Audiol. 47, S16–S20. http://dx.doi.org/10.1080/14992020802340116.
Näätänen, R., Paavilainen, P., Rinne, T., Alho, K., 2007. The mismatch negativity (MMN) in basic research of central auditory processing: a review. Clin. Neurophysiol. 118, 2544–2590. http://dx.doi.org/10.1016/j.clinph.2007.04.026.
Nelson, D.A., Lassman, F.M., 1968. Effects of intersignal interval on the human auditory evoked response. J. Acoust. Soc. Am. 44, 1529–1532. http://dx.doi.org/10.1121/1.1911292.
Nikjeh, D.A., Lister, J.J., Frisch, S.A., 2009. Preattentive cortical-evoked responses to pure tones, harmonic tones, and speech: influence of music training. Ear Hear 30, 432–446.
Nwabueze-Ogbo, F.C., Popelar, J., Syka, J., 2002. Changes in the acoustically evoked activity in the inferior colliculus of the rat after functional ablation of the auditory cortex. Physiol. Res. 51, S95–S104.
Pantev, C., Bertrand, O., Eulitz, C., Verkindt, C., Hampson, S., Schuierer, G., Elbert, T., 1995. Specific tonotopic organizations of different areas of the human auditory cortex revealed by simultaneous magnetic and electric recordings. Electroencephalogr. Clin. Neurophysiol. 94, 26–40. http://dx.doi.org/10.1016/0013-4694(94)00209-4.
Parbery-Clark, A., Anderson, S., Hittner, E., Kraus, N., 2012. Musical experience offsets age-related delays in neural timing. Neurobiol. Aging 33, 1483. http://dx.doi.org/10.1016/j.neurobiolaging.2011.12.015 e1-1483.e4.
Penhune, V.B., Zatorre, R.J., MacDonald, J.D., Evans, A.C., 1996. Interhemispheric anatomical differences in human primary auditory cortex: probabilistic mapping and volume measurement from magnetic resonance scans. Cereb. Cortex 6, 661–672. http://dx.doi.org/10.1093/cercor/6.5.661.
Peruzzi, D., Sivaramakrishnan, S., Oliver, D.L., 2000. Identification of cell types in brain slices of the inferior colliculus. Neuroscience 101, 403–416. http://dx.doi.org/10.1016/S0306-4522(00)00382-1.
Picton, T.W., Alain, C., Otten, L., Ritter, W., Achim, A., 2000. Mismatch negativity: different water in the same river. Audiol. Neurotol. 5, 111–139.
Picton, T.W., Alain, C., Woods, D.L., John, M.S., Scherg, M., Valdes-Sosa, P., Bosch-Bayard, J., Trujillo, N.J., 1999. Intracerebral sources of human auditory-evoked potentials. Audiol. Neurootol. 4, 64–79.
Picton, T.W., Woods, D.L., Baribaeu-Braun, J., Healy, T.M.G., 1977. Evoked potential audiometry. J. Otolaryngol. 6, 90–119.
Plourde, G., Garcia-Asensi, A., Backman, S., Deschamps, A., Chartrand, D., Fiset, P., Picton, T.W., 2008. Attenuation of the 40-Hz auditory steady state response by propofol involves the cortical and subcortical generators. Anesthesiology 108, 233–242.
Polich, J., 2007. Updating P300: an integrative theory of P3a and P3b. Clin. Neurophysiol. 118, 2128–2148. http://dx.doi.org/10.1016/j.clinph.2007.04.019.
Regan, D., Regan, M.P., 1988. The transducer characteristic of hair cells in the human ear: a possible objective measure. Brain Res. 438, 363–365. http://dx.doi.org/10.1016/0006-8993(88)91364-9.
Ross, B., Borgmann, C., Draganova, R., Roberts, L.E., Pantev, C., 2000. A high-precision magnetoencephalographic study of human auditory steady-state responses to amplitude-modulated tones. J. Acoust. Soc. Am. 108, 679–691.
Ross, B., Draganova, R., Picton, T.W., Pantev, C., 2003. Frequency specificity of 40-Hz auditory steady-state responses. Hear. Res. 186, 57–68. http://dx.doi.org/10.1016/S0378-5955(03)00299-5.
Ross, B., Picton, T.W., Pantev, C., 2002. Temporal integration in the human auditory cortex as represented by the development of the steady-state magnetic field. Hear. Res. 165, 68–84.
Ross, B., Tremblay, K., 2009. Stimulus experience modifies auditory neuromagnetic responses in young and older listeners. Hear. Res. 248, 48–59. http://dx.doi.org/10.1016/j.heares.2008.11.012.
Russo, N.M., Nicol, T.G., Zecker, S.G., Hayes, E.A., Kraus, N., 2005. Auditory training improves neural timing in the human brainstem. Behav. Brain Res. 156, 95–103. http://dx.doi.org/10.1016/j.bbr.2004.05.012.
Shahin, A., Bosnyak, D.J., Trainor, L.J., Roberts, L.E., 2003. Enhancement of neuroplastic P2 and N1c auditory evoked potentials in musicians. J. Neurosci. 23, 5545–5552.
Shiga, T., Althen, H., Cornella, M., Zarnowiec, K., Yabe, H., Escera, C., 2015. Deviance-related responses along the auditory hierarchy: combined FFR, MLR and MMN evidence. PLOS ONE 10, e0136794. http://dx.doi.org/10.1371/journal.pone.0136794.
Skoe, E., Kraus, N., 2013. Musical training heightens auditory brainstem function during sensitive periods in development. Front. Psychol. 4 http://dx.doi.org/10.3389/fpsyg.2013.00622.
Skoe, E., Kraus, N., 2010a. Auditory brainstem response to complex sounds: a tutorial. Ear Hear 31, 302–324. http://dx.doi.org/10.1097/AUD.0b013e3181cdb272.
Skoe, E., Kraus, N., 2010b. Hearing it again and again: on-line subcortical plasticity in humans. PLOS ONE 5, e13645. http://dx.doi.org/10.1371/journal.pone.0013645.
Skoe, E., Krizman, J., Spitzer, E., Kraus, N., 2013. The auditory brainstem is a barometer of rapid auditory learning. Neuroscience 243, 104–114. http://dx.doi.org/10.1016/j.neuroscience.2013.03.009.
Smith, J.C., Marsh, J.T., Brown, W.S., 1975. Far-field recorded frequency-following responses: evidence for the locus of brainstem sources. Electroencephalogr. Clin. Neurophysiol. 39, 465–472. http://dx.doi.org/10.1016/0013-4694(75)90047-4.
Smith, J.C., Marsh, J.T., Greenberg, S., Brown, W.S., 1978. Human auditory frequency-following responses to a missing fundamental. Science 201, 639–641.
Sohmer, H., Feinmesser, M., 1970. Cochlear and cortical audiometry conveniently recorded in the same subject. Isr. J. Med. Sci. 6, 219–223.
Sohmer, H., Pratt, H., Kinarti, R., 1977. Sources of frequency following responses (FFR) in man. Electroencephalogr. Clin. Neurophysiol. 42, 656–664. http://dx.doi.org/10.1016/0013-4694(77)90282-6.
Song, J.H., Skoe, E., Wong, P.C., Kraus, N., 2008. Plasticity in the adult human auditory brainstem following short-term linguistic training. J. Cogn. Neurosci. 20, 1892–1902.
Suga, N., 2008. Role of corticofugal feedback in hearing. J. Comp. Physiol. A 194, 169–183. http://dx.doi.org/10.1007/s00359-007-0274-2.
Suga, N., Gao, E., Zhang, Y., Ma, X., Olsen, J.F., 2000. The corticofugal system for hearing: recent progress. Proc. Natl. Acad. Sci. 97, 11807–11814.
Suga, N., Ma, X., 2003. Multiparametric corticofugal modulation and plasticity in the auditory system. Nat. Rev. Neurosci. 4, 783–794. http://dx.doi.org/10.1038/nrn1222.
Suga, N., Xiao, Z., Ma, X., Ji, W., 2002. Plasticity and corticofugal modulation for hearing in adult animals. Neuron 36, 9–18. http://dx.doi.org/10.1016/S0896-6273(02)00933-9.
Suzuki, Y., 2000. Contribution of cochlear nucleus to 80 Hz amplitude-modulation following response. Nippon. Jibiinkoka Gakkai Kaiho 103, 177–187.
Thornton, A.R.D., 2007. Instrumentation and recording parameters. In: Burkard, R.F., Eggermont, J.J., Don, M. (Eds.), Auditory Evoked Potentials: Basic Principles and Clinical Application. Lippincott Williams & Wilkins, Philadelphia, PA, pp. 42–47.
Tietze, G., 1979. Stimulation methods for simultaneous derivation of acoustically evoked brainstem and cortical responses. Scand. Audiol. Suppl. 11, 97–104.
Tonnquist-Uhlén, I., Borg, E., Persson, H.E., Spens, K.E., 1996. Topography of auditory evoked cortical potentials in children with severe language impairment: the N1 component. Electroencephalogr. Clin. Neurophysiol. Evoked Potentials Sect. 100, 250–260. http://dx.doi.org/10.1016/0168-5597(95)00256-1.
Tremblay, K., Kraus, N., McGee, T., Ponton, C., Otis, B., others, 2001. Central auditory plasticity: changes in the N1-P2 complex after speech-sound training. Ear Hear 22, 79–90.
Tremblay, K.L., Kraus, N., 2002. Auditory training induces asymmetrical changes in cortical neural activity. J. Speech Lang. Hear. Res. 45, 564–572.
Tremblay, K.L., Piskosz, M., Souza, P., 2002. Aging alters the neural representation of speech cues. Neuroreport 13, 1865–1870.
Uther, M., Kujala, A., Huotilainen, M., Shtyrov, Y., Näätänen, R., 2006. Training in Morse code enhances involuntary attentional switching to acoustic frequency: evidence from ERPs. Brain Res. 1073–1074, 417–424. http://dx.doi.org/10.1016/j.brainres.2005.12.047.
Wier, C.C., Jesteadt, W., Green, D.M., 1977. Frequency discrimination as a function of frequency and sensation level. J. Acoust. Soc. Am. 61, 178–184. http://dx.doi.org/10.1121/1.381251.
Winer, J.A., 2005. Decoding the auditory corticofugal systems. Hear. Res. 207, 1–9. http://dx.doi.org/10.1016/j.heares.2005.06.007.
Winkler, I., Tervaniemi, M., Näätänen, R., 1997. Two separate codes for missing-fundamental pitch in the human auditory cortex. J. Acoust. Soc. Am. 102, 1072. http://dx.doi.org/10.1121/1.419860.
Wong, P.C.M., Skoe, E., Russo, N.M., Dees, T., Kraus, N., 2007. Musical experience shapes human brainstem encoding of linguistic pitch patterns. Nat. Neurosci. 10, 420–422. http://dx.doi.org/10.1038/nn1872.
Woods, D.L., Alain, C., Covarrubias, D., Zaidel, O., 1993. Frequency-related differences in the speed of human auditory processing. Hear. Res. 66, 46–52. http://dx.doi.org/10.1016/0378-5955(93)90258-3.
Worden, F.G., Marsh, J.T., 1968. Frequency-following (microphonic-like) neural responses evoked by sound. Electroencephalogr. Clin. Neurophysiol. 25, 42–52. http://dx.doi.org/10.1016/0013-4694(68)90085-0.
Wu, Y., Yan, J., 2007. Modulation of the receptive fields of midbrain neurons elicited by thalamic electrical stimulation through corticofugal feedback. J. Neurosci. 27, 10651–10658. http://dx.doi.org/10.1523/JNEUROSCI.1320-07.2007.
Yamaguchi, S., Knight, R.T., 1991. P300 generation by novel somatosensory stimuli. Electroencephalogr. Clin. Neurophysiol. 78, 50–55. http://dx.doi.org/10.1016/0013-4694(91)90018-Y.
Zendel, B.R., Alain, C., 2014. Enhanced attention-dependent activity in the auditory cortex of older musicians. Neurobiol. Aging 35, 55–63. http://dx.doi.org/10.1016/j.neurobiolaging.2013.06.022.
Zhou, X., Jen, P.H.-S., 2007. Corticofugal modulation of multi-parametric auditory selectivity in the midbrain of the big brown bat. J. Neurophysiol. 98, 2509–2516. http://dx.doi.org/10.1152/jn.00613.2007.
Zurek, P.M., 1992. Detectability of transient and sinusoidal otoacoustic emissions. Ear Hear 13, 307–310.